SSRv manuscript No.
(will be inserted by the editor)

GeV Particle Acceleration in Solar Flares and Ground Level Enhancement (GLE) Events

Markus J. Aschwanden[1]

Received: 2010-Apr-30 / Accepted: ...

Abstract *Ground Level Enhancement (GLE)* events represent the largest class of *solar energetic particle (SEP)* events that require acceleration processes to produce $\gtrsim 1$ GeV ions in order to produce showers of secondary particles in the Earth's atmosphere with sufficient intensity to be detected by ground-level neutron monitors, above the background of cosmics rays. Although the association of GLE events with solar flares and coronal mass ejections (CMEs) is unambiguous, the question arises about the location of the responsible acceleration site: coronal flare sites or interplanetary CME-associated shocks? To answer this question we scrutinize the timing of GLE events with respect to hard X-ray production in solar flares, the height and magnetic morphology of active regions, the role of extended acceleration and particle trapping, as well as the maximum observed energies in solar gamma rays. We conclude that 70% of most recent 13 GLE events are consistent with acceleration during the impulsive flare phase, while the remaining 30% could be subject to extended acceleration and trapping, or partially originate in CME-associated shocks.

Keywords Solar Flares — Particle Acceleration — Ground Level Enhancements

1 Introduction

A key aspect that motivated this review is the question whether *ground level enhancement (GLE)* events, which apparently require acceleration processes that produce $\lesssim 1$ GeV particles, originate from flare regions in the solar corona or from coronal mass ejections while propagating through the interplanetary space. GLE events represent the largest *solar energetic particle (SEP)* events that accelerate GeV ions with sufficient intensity so that secondary particles are detected by ground-level neutron monitors above the galactic cosmic-ray background (Reames 2009b). A catalog of 70 GLE events, occurring during the last six solar cycles from 1942 to 2006, has been compiled (Cliver et

[1]) Solar & Astrophysics Laboratory, Lockheed Martin Advanced Technology Center, Bldg. 252, Org. ADBS, 3251 Hanover St., Palo Alto, CA 94304, USA
Tel.: +650-424-4001
Fax: +650-424-3994
E-mail: aschwanden@lmsal.com

al. 1982; Cliver 2006), which serves as the primary database of many GLE studies. So, GLE events are very rare, occurring only about a dozen times per solar cycle, which averages to about one event per year. While GLE events with 1 GeV energies represent the largest energies produced inside our solar system, they are at the bottom of the cosmic ray spectrum, which covers an energy range of $\approx 10^9 - 10^{21}$ eV, exhibiting a "spectral knee" between particles accelerated inside our galaxy ($\approx 10^9 - 10^{16}$ eV) and in extragalactic sources ($\approx 10^{16} - 10^{21}$ eV).

In order to address our central question whether GeV particles producing GLE events are of solar or heliospheric origin, we will review various aspects of flare observations of GLE events, such as the relative timing of the release of GLE-associated particles during solar flares (Section 2.1), the height of acceleration regions (Section 2.2), the magnetic topology of solar flare acceleration regions (Section 2.3), the role of extended acceleration phases and particle trapping in solar flares (Section 2.4), and the maximum energies of gamma-ray producing particles in solar spectra (Section 2.5). We summarize our conclusions in Section 3. Complementary aspects of the same question from the view of CME-associated shocks are treated in the article of Guang Li, and active region characteristics of GLE-associated flares are reviewed by Nariaki Nitta in this volume.

2 Flare Observations of GLE Events

All GLE events are associated with solar flares of the most intense category (GOES X-class in virtually all cases). At the same time, *coronal mass ejections* (CME) were reported in all recent cases. Thus we can say that flares and CMEs are both necessary conditions for a GLE event, but it leaves us with the ambiguity where the acceleration of GeV particles reponsible for GLE events takes place. In the following we investigate and review various observational aspects of relevant flare data that could shed some light into this question.

2.1 Solar Particle Release Times

For the analysis of the timing of GLE events we are using solar release times that are normalized to the Earth-arrival times of electromagnetic signals, as compiled for 16 events during 1997-2006 (Gopalswamy et al. 2008; Reames 2009a) and for 30 events during 1973-2006 (Reames 2009b).

In Fig. 1 we display the time profiles of 13 events (out of the 16 GLE events occurring during 1994-2007) analyzed in Reames (2009a), for which the solar release time could be determined with the velocity dispersion method. The flare time profiles we show in Fig. 1 are the soft X-ray fluxes $I_{SXR}(t)$ detected by GOES in the soft (1-8 Å) and hard (0.5-4 Å) channel (thin solid and dashed curves), as well as their time derivatives (thick solid and dashed curves), which are generally considered as a good proxi of the hard X-ray flux $I_{HXR}(t)$,

$$I_{HXR}(t) \approx \frac{dI_{SXR}(t)}{dt} \ , \tag{1}$$

according to the Neupert effect (Neupert 1968; Hudson 1991; Dennis and Zarro 1993; see also Section 13.5.5 in Aschwanden 2004 and references therein). Note that the time

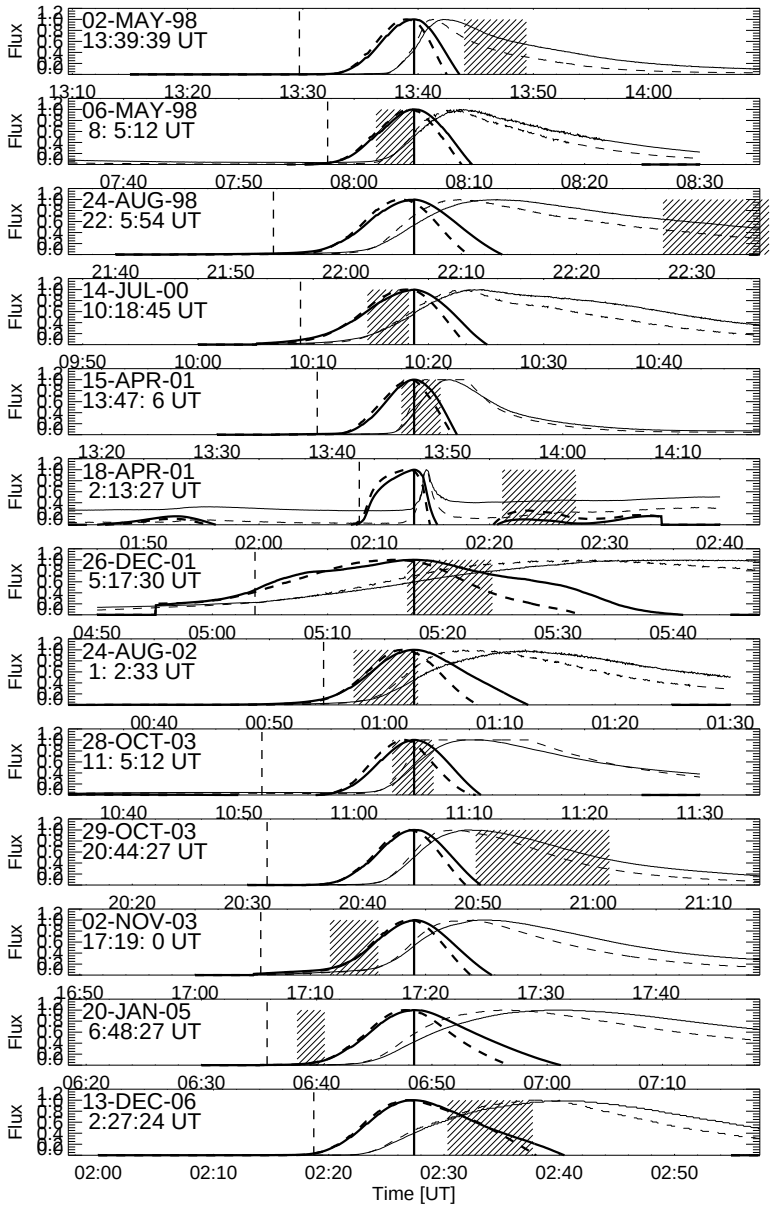

Fig. 1 Time profiles of the GOES 1-8 Å soft X-ray fluxes (solid curve), GOES 0.5-4 Å fluxes (dashed curve), and their time derivatives (thick curves), which are a proxi for the hard X-ray flux, and solar particle release times with uncertainties (hashed areas) of 13 GLE events during 1998-2006. The time range is centered at the hard X-ray peak time (given on the left side). The *solar particle release times (SPR)* are determined from the velocity dispersion of particles detected with WIND by Reames (2009b). The start times of radio type II bursts are indicated with vertical dashed bars.

Table 1 Timing of 13 GLE events during 1998-2006.

GLE	Date	Type II start time t_{II} [UT]	Hard X-ray peak time t_{HXR} [UT]	SPR time t_{SPR} [UT]	Delay SPR-II [min]	Delay SPR-HXR [min]	Location	Refs.
56	1998-May-02	13:29.42	13:39:39	13:46:42	17.0±2.7	+8.1	S15W15	1,2-5
57	1998-May-06	07:57.42	08:05:12	08:03:30	5.8±1.6	-1.7	S15W64	1
58	1998-Aug-24	21:53.42	22:05:54	22:32:06	38.4±4.6	+26.2	N35E09	1
59	2000-Jul-14	10:08.54	10:18:45	10:16:30	7.6±1.8	-2.3	N22W07	1,6-8
60	2001-Apr-15	13:38.42	13:47:06	13:47:42	9.0±1.7	+0.6	S20W84	1,7
61	2001-Apr-18	02:08.42	02:13:27	02:24:18	15.6±3.2	+10.9	≈W115	1
63	2001-Dec-26	05:03.42	05:17:30	05:20:36	16.9±3.7	+3.1	N08W54	1
64	2002-Aug-24	00:54.42	01:02:33	01:00:06	5.4±2.8	-2.5	S02W81	1
65	2003-Oct-28	10:52.00	11:05:12	11:05:06	13.1±1.8	-0.1	S16E08	1,9-12
66	2003-Oct-29	20:31.42	20:44:27	20:55:36	23.9±5.8	+11.2	S15W02	1,10
67	2003-Nov-02	17:05.42	17:19:00	17:13:48	8.1±2.1	-5.2	S14W56	1,10
69	2005-Jan-20	06:35.42	06:48:27	06:39:30	3.8±1.2	-9.0	N12W58	1,12,14-23
70	2006-Dec-13	02:18.42	02:27:24	02:34:00	15.3±3.7	+6.6	S06W26	1,24-25

References: 1) Reames et al. 2009b; 2) Shumilov et al. 2003; 3) Torsti et al. 2004; 4) Pohjolainen et al. 2001; 5) Kocharov et al. 2006; 6) Li et al. 2007; 7) Vashenyk et al. 2003; 8) Aschwanden and Alexander 2001; Wang 2009; 9) Klassen et al. 2005; 10) Miroshnichenko 2004; 11) Watanabe et al. 2008; 12) Chupp and Ryan 2009; 13) Grechnev et al. 2008; 14) Kuznetsov et al. 2006; 15) Masson and Klein 2009; 16) Simnett 2006, 2007; 17) Simnett an Roelof 2005a,b; 18) Bombardieri et al. 2008; 19) McCracken et al. 2008; 20) Wang and Wang 2006; 21) Moraal et al. 2008; 22) Martirosyan and Chilingarian 2005; 23) Matthiä et al. 2009; 24) Bieber et al. 2008; 25) Li et al. 2009.

derivatives of both soft X-ray channels yield a near-simultaneous hard X-ray peak time ($\ll 1$ min) within the accuracy needed here. The time profiles shown in Fig. 1 are all of the same length (1 hr) and centered at the hard X-ray peak time t_{HXR}, which we consider as the reference time for acceleration of the most energetic particles during a flare. The physical explanation for the Neupert effect is that the hard X-ray peak time coincides with the time of most intense precipitation of accelerated high-energy particles down to the chromosphere (within a time-of-flight interval of $\approx 10-100$ ms), which represents the time interval of most intense heating of chromospheric plasma, giving rise to the steepest increase of the soft X-ray flux during a flare. These hard X-ray peak times t_{HXR} are listed in Table 1, which typically occur about $\approx 5-10$ min after the soft X-ray onset times, but preceed the soft X-ray peak times by about 1-15 min. The start or peak of soft X-ray emission (as listed in GOES flare catalogs) should not be used as a reference time for particle acceleration, because they rather bracket the beginning and end of significant hard X-ray emission and the concomitant acceleration phase.

The *solar particle release times* t_{SPR} on the other hand, were measured from the velocity dispersion of particles arriving at ground-based neutron monitors or at particle detectors in near-Earth satellites, such as with the *Interplanetary Monitoring Platform 8 (IMP-8)* and the *WIND* spacecraft (Reames 2009a,b). An example of such a measurement is shown in Fig. 2 for the GLE event of 1978 May 7. A plot of the arrival time versus the reciprocal velocity ($1/v$) shows a nearly-linear relationship that can be fitted with a linear regression fit and yields the path length ($\approx 1.1-2.1$ AU) as well as the so-called *solar particle release time* t_{SPR} within an accuracy of typically $\pm 1, ..., 3$ min. We list these extrapolated solar particle release times t_{SPR} determined by Reames (2009a) in Table 1 and mark their range of uncertainty with a hashed area in Fig. 1. Interestingly, about half (6 out of the 13 cases) overlap with the hard X-ray

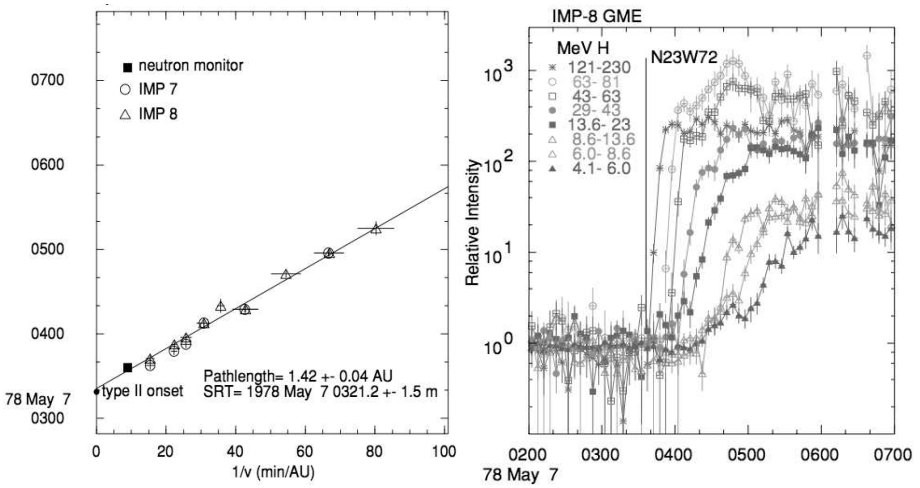

Fig. 2 Example of a velocity dispersion measurement of GLE arrival times of protons at IMP-7, IMP-8, or neutron monitors (y-axis in left panel) versus the reciprocal velocity ($1/v$) (x-axis in left plot), which allows to extrapolate the energy release time t_{SPR} at the source location ($1/v \mapsto 0$), for the GLE event of 1978 May 7. The timing of the relative intensity of the protons with different energies is shown in the right-hand-side panel (Reames 2009b).

peak time t_{HXR}, while two cases coincide with the start of hard X-rays, and one case occurs during the decay of hard X-rays. Only four cases occur after the hard X-rays ceased. Therefore, we can say that $\approx 70\%$ (9 out of 13) of the GLE events are consistent with flare acceleration, while $\approx 30\%$ occur significantly delayed (by $\approx 10-30$ min) and could be consistent with acceleration in CMEs, based on the relative timing to hard X-rays. This results is not inconsistent with an earlier review by Cliver et al. (1982), where the most likely injection onset of GeV protons was found to conincide with the first significant microwave peak (which is produced by gyrosynchrotron emission and generally coincides with the production of nonthermal hard X-rays). Another timing indicator is the onset time t_{II} of metric type II bursts, which is also listed in Table I (from Gopalswamy et al. 2008). The onset of type II bursts indicate the formation of a CME-related shock front. These type II onset times t_{II} are indicated with a dashed vertical bar in Fig. 1, which all seem to coincide with the very start of significant soft X-ray or hard X-ray emission. Apparently, shocks form in these intense X-class flares very early on due to the high speed of the CME front, about at the same time when the magnetic field becomes stretched out below the erupting filament, which triggers magnetic reconnection, particle acceleration, and chromospheric hard X-ray and soft X-ray emission subsequently. Apparently, the solar particle release times t_{SPR} occur always later (Fig. 1), and thus we cannot exclude that the particles responsible for GLE events could also be accelerated in the CME-related shock fronts, based on the onset times t_{II} of radio type II bursts.

One GLE event, for which the timing was most extensively determined is the second-latest event of 2005 Jan 25. The steepest increase of the soft X-ray flux occurs around 06:48 UT (Fig. 1). Hard X-ray time profiles from RHESSI show a peak of the 50-100 keV and 300-800 keV emission around 06:45-06:46 UT, while the gamma-ray emission at 2-6 MeV, 23-40 MeV, and > 60 MeV detected with SONG peak around 06:46-06:47 UT (Kuznetsov et al. 2006; Grechnev et al. 2008). The solar particle release

time was determined at 06:39 UT (Reames 2009a), about 6-8 min earlier than the hard X-ray and gamma-ray peaks, and about 3 min after the type II start time at 06:36 UT. Based on the temporal and spectral properties it was concluded that the acceleration site leading to the SEP/GLE spike is likely to be located in the flare region rather than in CME shocks, at least for the leading SEP/GLE spike (Grechnev et al. 2008; Simnett and Roelof 2005a, 2005b; Simnett 2006, 2007; Kuznetsov et al. 2006; Wang and Wang 2006; Bombardieri et al. 2008; Chupp and Ryan 2009; Masson and Klein 2009), while a second component later on could be accelerated in a CME-associated shock at a distance of $\approx 3-5$ solar radii (McCracken et al. 2008; McCracken and Moraal 2008; Moraal et al. 2008).

2.2 Height of Acceleration Region

After we established the temporal coincidence of particle acceleration with flare hard X-ray emission (in 70% of the GLE events), we turn now to the question of the spatial localization.

One method to estimate the height of the acceleration region of GLE particles (Reames 2009a,b) is based on an assumed height h_{II} of the start of radio type II bursts, corrected for the propagation delay of the CME shock front with speed v_{CME} during the time interval $\Delta t = t_{SPR} - t_{II}$ between the start t_{II} of the radio type II burst and the solar particle release time t_{SPR},

$$h_{SPR} = h_{II} + v_{CME}(t_{SPR} - t_{II}) \ , \tag{2}$$

which is always higher than h_{II}, because $v_{CME} > 0$ and $t_{SPR} > t_{II}$. Reames (2009a,b) assumed a nominal average height of $h_{SPR} = 1.5 \pm 0.5$ solar radii based on standard coronal density models $n_e(h)$ and statistical start frequencies of type II bursts around $\nu \approx 100$ MHz (Kundu 1965), which corresponds to an electron density of $n_e \approx 10^8$ cm^{-3} in the case of fundamental plasma emission, i.e., $f_{pe} \approx 8980\sqrt{n_e}$. Taking the propagation delay of $(t_{SPR} - t_{II}) \approx 5-15$ min and the CME speeds of $v_{CME} \approx 1000-3000$ km s^{-1} into account, Reames (2009a,b) arrived at estimated heights of $h_{SPR} \approx 2-5$ solar radii, with a possible dependence on the heliographic longitude. This method implicitly assumes that particles are accelerated in CME shocks, whose location is entirely tied to the height and propagation speed of the type II and CME shock front, which certainly is a reasonable explanation for those 30% of GLE events that exhibit a starting time t_{SPR} significantly delayed to the hard X-ray emission.

Alternatively, since 70% of the GLE events exhibit a starting time t_{SPR} during the phase of hard X-ray emission, we can estimate the height of their acceleration region from the hard and soft X-ray data. The mildly relativistic electrons accelerated in a flare exhibit a time-of-flight delay between their coronal acceleration site and the chromospheric target region where bright hard X-ray emission is observed, depending on their kinetic energy. From the velocity dispersion of these energy-dependent hard X-ray time delays, the propagation distance and height of the acceleration region can be calculated, with proper correction for the geometry of the trajectory and for the pitch angles of the particles.

For a GLE precursor flare, which occurred on 1992 June 25, 17:32 UT (hard X-ray start time) at heliographic position N10/W75, such a time-of-flight measurement is available (Fig. 3), based on Yohkoh/HXT and SXT observations (Aschwanden et al. 1996). This flare is of the GOES M1.4-class and peaked in soft X-rays at 17:54 UT.

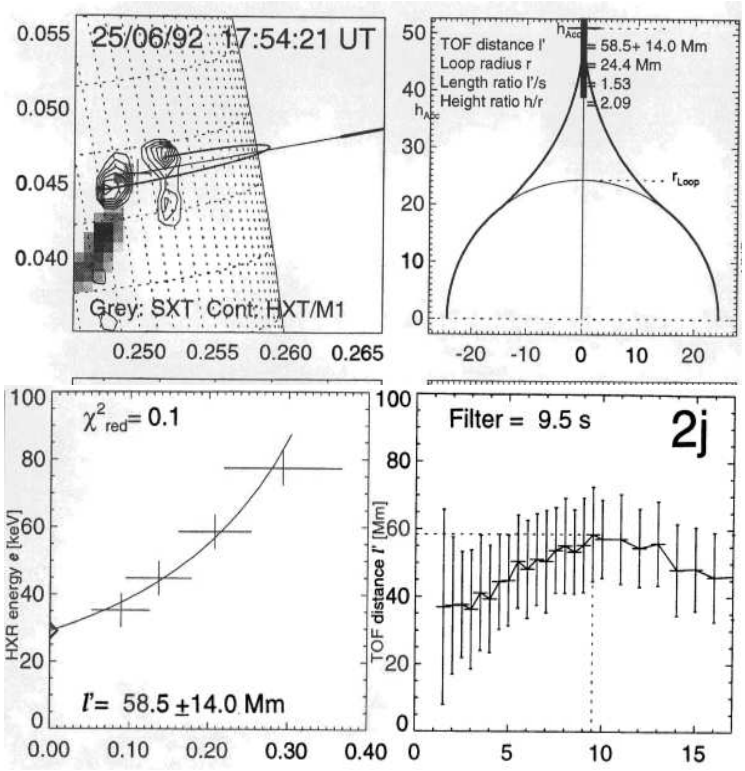

Fig. 3 Altitude measurement of the acceleration source during the 1992 June 25 GLE precursor flare based on the velocity dispersion of electron time-of-flight delays, measured with the *Compton Gamma Ray Observatory (CGRO)*, *Yohkoh/HXT*, and *SXT*. A hard X-ray image from HXT/M1 (23-33 keV) of the flare footpoint sources (contours) and a SXT soft X-ray image from Yohkoh/SXT (greyscale) are shown in the top left panel. The energy-dependent hard X-ray time delays in the range of $\Delta t \lesssim 300$ ms are shown in the bottom left panel, yielding a time-of-flight distance of $L' = 58.5 \pm 14.0$ Mm, which is projected onto the inferred loop geometry (top right panel). The uncertainty of the TOF distance is derived from varying the filter time scale (bottom right panel), (Aschwanden et al. 1996).

Concomitant hard X-ray and radio emission is also studied in Wang et al. (1995), finding a spatial separation of 35 Mm between the simultaneous hard X-ray and microwave emission, which provides also an approximate scale for the horizontal and vertical extent of the flare region. This flare is a precursor to a GLE event 2 hrs later at the same location, which is listed as GLE event # 53 in Cliver (2006), peaking at 20:14 UT at position N10/W68, and is classified as X3 GOES-class flare. We can consider the two rapidly following events as *homologous flares* within the same active region that are likely to have a similar magnetic configuration. The time-of-flight distance for the precursor flare was evaluated from the time delay τ_{ij} between electrons with relativistic speeds of β_i and β_j in the hard X-ray photon energy range of $\epsilon \approx 20 - 80$ keV,

$$l_{TOF} = c\tau_{ij} \left(\frac{1}{\beta_i} - \frac{1}{\beta_j} \right)^{-1} \quad , \tag{3}$$

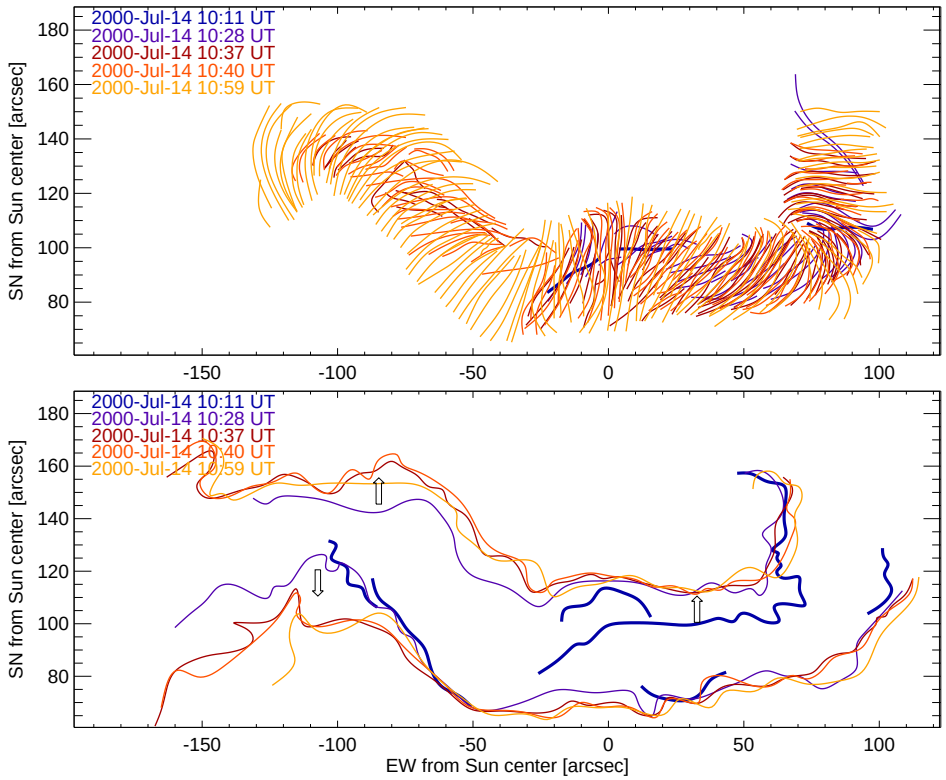

Fig. 4 *Top:* tracings of individual flare loops from *TRACE* 171 Å images of the Bastille-Day flare 2000-Jul-14. The five sets of loops traced at five different times are marked with different greytones. Note the evolution from highly sheared to less sheared loops. *Bottom:* the position of the two flare ribbons traced from 171 Å images. Note the increasing footpoint separation with time (Aschwanden 2002).

which after correction for electron pitch angle, helical twist of field lines, and projection effects of loop size yielded a value of $L' = 58.5 \pm 14.0$ Mm, corresponding to a height of $h \approx 50 \pm 13$ Mm. This is a fairly typical height of the acceleration region for large flares, amounting to about the double height of the soft X-ray loops. From statistics of 42 flares, an average height ratio of $h/h_{loop} \approx L/L_{loop} = 1.4 \pm 0.3$ was obtained (Aschwanden et al. 1996), for flare loop radii of $r_{loop} \approx 2 - 20$ Mm. Thus, the height range of acceleration regions in flares amounts to $h \approx 4 - 40$ Mm, which corresponds to $\lesssim 5\%$ of a solar radius. In summary, since about 70% of the GLE events are consistent with a particle release time during the flare hard X-ray phase, they are also consistent with acceleration heights of $h \lesssim 0.05$ solar radii.

2.3 Magnetic Topology of Acceleration Region

The geometry and magnetic topology of a solar flare region has been studied in most detail for the GLE event of 2000 July 14, 10:18 UT, an X5.7 GOES-class flare (e.g., Aulanier et al. 2000; Aschwanden and Alexander 2001; Aschwanden 2002; Yan and

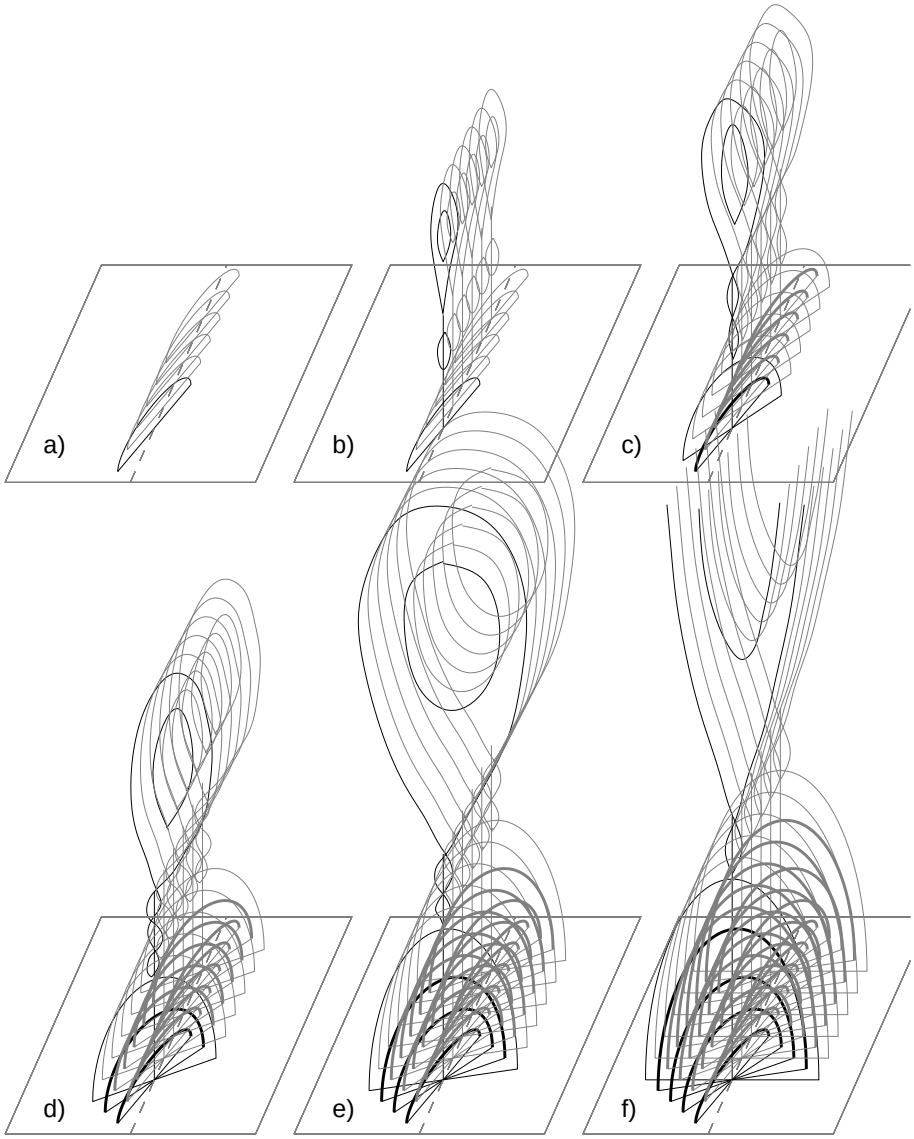

Fig. 5 Scenario of the dynamic evolution during the Bastille-Day 2000-Jul-14 flare: *(a)* low-lying, highly sheared loops above the neutral line become unstable first; *(b)* after loss of magnetic equilibrium the filament jumps upward and forms a current sheet according to the model by Forbes and Priest (1995). When the current sheet becomes stretched, magnetic islands form and coalescence of islands occurs at locations of enhanced resistivity, initiating particle acceleration and plasma heating; *(c)* the lowest lying loops relax after reconnection and become filled due to chromospheric evaporation (loops with thick linestyle); *(d)* reconnection proceeds upward and involves higher lying, less-sheared loops; *(e)* the arcade gradually fills up with hot flare loops; *(f)* the last reconnecting loops have no shear and are oriented perpendicular to the neutral line. At some point the filament disconnects completely from the flare arcade and escapes into interplanetary space (Aschwanden 2002).

Huang 2003; Aschwanden and Aschwanden 2008). The solar energy release times of the particles responsible for the GLE spike during the Bastille-Day flare is well-synchronized with the rise phase of hard X-ray emission (Fig. 1, Table 1; Reames 2009b; Li et al. 2007; Wang 2009). The Bastille-Day flare was observed near disk center, which provided an excellent view on the projected flare area, which consists of a classical double-ribbon structure as it is typical for most large flares. The double-ribbon structure straddles along a neutral line from east to west, and spreads apart as a function of time (Fig. 4, bottom), as expected in the *Carmichael- Sturrock- Hirayama-Kopp- Pneuman (CSHKP)* standard flare model. While the CSHKP model essentially describes the vertical evolution in a 2-D cross-section of the flare arcade, the Bastille-Day flare in addition shows also the horizontal projection and the 3-D evolution in detail. From loop tracings at different times during the flare (Fig. 4, top) it is evident that low-lying, highly-sheared loops over the neutral line brighten first, triggering a sequence of flare loops that progress to higher-lying and less-sheared field lines above the neutral line, until we see a final double-ribbon flare arcade at orthogonal angles to the neutral line, spanning over a width of $w \approx 50$ Mm in NS direction and a length of $l \approx 250$ Mm in EW direction. From this time evolution we can reconstruct the 3-D geometry of the magnetic field lines that are involved in the flare as shown in Fig. 5. Since the bright EUV postflare loops outline the relaxed field line configuration after magnetic reconnection, we can directly infer the size and height of the magnetic reconnection region, which, statistically, is located about a factor of 1.5 above the soft X-ray and EUV postflare loops (Aschwanden et al. 1996), estimated to be in an altitude of $h \approx w \approx 50$ Mm with a length of $l \approx 250$ Mm. This height range of the magnetic reconnection region confines the overall volume of the particle acceleration region, although a highly fragmentated structure with many magnetic islands is expected, caused by the tearing-mode instability and bursty reconnection (e.g., Sturrock 1966; Karpen et al. 1995, 1998; Kliem et al. 2000; Shibata and Tanuma 2001).

Some consequences of this magnetic topology for GLE events are: (1) The vertical X-type reconnection geometry allows particle acceleration in upward and downward direction in a quasi-symmetric fashion, so that particles of almost equal energies can be accelerated in both directions; (2) The magnetic field lines above the vertical current sheet of the main reconnection regions are likely to be open, which allows escape of accelerated particles into interplanetary space and along Earth-connected magnetic field lines; (3) The relatively low height in the solar corona ($h \lesssim 50$ Mm) provides a large reservoir of thermal particles that can be accelerated in sufficient numbers that are necessary for GLE detection. The escape conditions of accelerated particles into interplanetary space requires open magnetic field lines, which exist not only in coronal holes but also to a substantial fraction in active regions. Schrijver and DeRosa (2003) found from potential-field extrapolations of the global magnetic field over the entire solar surface that the interplanetary magnetic field (IMF) originates typically in a dozen disjoint regions, around the solar cycle maximum. While active regions are often ignored as a source for the interplanetary magnetic field, Schrijver and DeRosa (2003) found that the fraction of the IMF that connects directly to magnetic plages of active regions increases from $\lesssim 10\%$ at cycle minimum up to $30-50\%$ at cycle maximum, with even direct connections between sunspots and the heliosphere. Evidence for open-field escape routes was demonstrated with magnetic field modeling, for instance for GLE event #70, 2006 Dec 13, 02:27 UT (Li et al. 2009). In flaring regions that expell a CME, particles accelerated in the reconnection region behind the rising filament may be trapped inside the CME bubble and cannot directly escape into interplanetary space (Reames 2002),

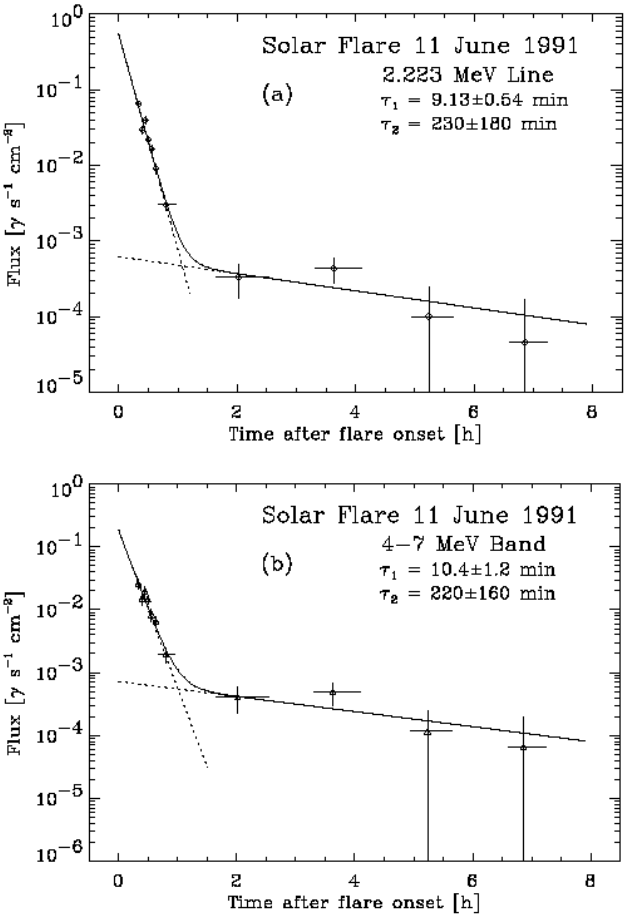

Fig. 6 Extended γ-ray emission as measured by *COMPTEL* for the GLE event #51 on 1991-Jun-11 flare in the 2.223 MeV neutron capture line (top) and the $4-7$ MeV nuclear line flux (bottom). The data have been corrected for primary and secondary bremsstrahlung. A two-fold exponential decay has been fitted. The origin of the time axis is 01:56 UT, and the flare onset reported by GOES. Only data of the extended phase (after 02:13 UT) are shown (Rank et al. 2001).

but may contribute to a seed population for secondary acceleration in CME-associated shocks (McCracken and Moraal 2008). The two populations of directly-escaping and trapped-plus-accelerated particles may be distinguishable as impulsive and gradual phases of SEP events.

2.4 Extended Particle Acceleration and Trapping

The solar particle release time t_{SPR} as determined by Reames (2009b) occurs after the main hard X-ray production phase in 5 cases out of the 13 recent GLE events listed in Table 1 and shown in Fig. 1, with a delay of $t_{SPR} - t_{HXR} \approx 6 - 11$ min in 4 cases, and ≈ 26 for the most extreme case. The question arises whether we can exclude an

interpretation in terms of a flare acceleration site for these 5 cases. If the flare site shows, besides the impulsive hard X-ray phase, also prolonged time intervals with hard X-ray and gamma-ray emission, either an extended (second-step) acceleration phase or extended trapping is possible, in which case the particles responsible for GLE signatures could possibly be accelerated at the coronal flare site rather than in interplanetary CME shocks. Extended acceleration can be diagnosed from impulsive bursts in hard X-ray, gamma-ray, and radio emission after the impulsive phase, while indicators of extended trapping are: (1) exponential decay of X-ray and gamma-ray light curves, (2) spectral hardening in hard X-rays (Kiplinger 1995; Grayson et al. 2009), or (3) type IV continuum emission in microwaves (produced by gyro-synchrotron emission from trapped high-relativistic electrons). Particle trapping times are limited by the collisional deflection time, which is for electrons

$$t_{trap}(\varepsilon) \lesssim t_{defl}(\varepsilon) = 0.95 \left(\frac{\varepsilon}{100\ \mathrm{keV}}\right)^{3/2} \left(\frac{10^{11}\ \mathrm{cm}^{-3}}{n_e}\right) \left(\frac{20}{\ln \Lambda}\right) \quad (s)\ , \qquad (4)$$

and a factor of ≈ 60 longer for ions. Postflare loops usually expand slowly with height, so that the density drops continuously and collisional deflection times (and thus trapping times) become progressively longer. Particle densities in the upper corona drop below $n_e \lesssim 10^8$ cm^{-3}, which enables trapping times over several hours.

The second diagnostic of extended acceleration, the spectral hardening after the impulsive phase, has recently been demonstrated with RHESSI to be a reliable predictor of SEP events (Grayson et al. 2009). From a dataset of 37 magnetically well-connected flares, 12 out of 18 flares with spectral soft-hard-harder (SHH) evolution produced SEP events, and none of the 19 flares without SHH behavior produced SEPs. Three of the 37 analyzed SEP events are GLE events and show all SHH behavior. This demonstrates a statistically significant correlation between SHH and SEP (and GLE) observations. Since the spectral hardening happens in the hard X-rays sources at the solar flare site, as imaged by RHESSI, this link between SHH and SEP is unexplained in the standard scenario of SEP acceleration in CME-related shocks during interplanetary propagation.

Extended gamma-ray emission with exponential decay times has indeed been observed up to 5-8 hours after the impulsive phase of the GLE event #51 on 1991 Jun 11 (Fig. 6) and GLE event #52 on 1991 Jun 15 (Kanbach et al. 1993; Rank et al. 1996, 2001). Evidence for prolonged acceleration of high-energy protons ($E > 100$ MeV) accelerated in flares and postflare loop systems, with associated spectral hardening late in the flare, was also discussed for GLE event #52, 1991 Jun 15, 08:17 UT (Chertok 1995), for GLE event #55, 1997 Nov 6, 11:55 UT (Klein and Trottet 2001; Murphy et al. 2001; Masuda 2002; Masuda and Sato 2003), for GLE event #59, 2000 Jul 14, 10:24 UT (Livshits and Belov 2004; Li et al. 2007; Wang 2009), and for GLE event #70, 2006 Dec 13, 02:27 UT (Li et al. 2009). Evidence for extended particle acceleration in the lower corona was also demonstrated from microwave gyro-resonance emission, requiring high magnetic fields near sunspots, e.g., for GLE event #69, 2005 Jan 20, 06:48 UT (Grechnev et al. 2008; Masson and Klein 2009). The GLE event #65 on 2003 Oct 28, 11:05 UT, shows multiple phases of impulsive particle injections, ending with a gradual phase (> 1 hr) of type III bursts that starts 25 min after the first type III bursts (Klassen et al. 2005; Miroshnichenko et al. 2004).

Let us also review the 5 recent GLE events listed in Table 1 that exhibit a delayed solar particle release time t_{SPR}. The GLE event #56 on 1998 May 02, 13:38 UT, has a delay of $t_{SPR} - t_{HXR} = +8.1$ min, at a time when the impulsive flare phase is over, but the radio dynamic spectra from Artemis IV show type IV continuum

Table 2 Hard X-ray and gamma-ray emission mechanisms operating in large solar flares, with observed photon energy and primary particle energy ranges (adapted from Ramaty and Mandzhavidze 1994)

Process	Observed photon energies	Primary particle energies
Bremsstrahlung continuum	20 keV−11 MeV	20 keV−1 MeV
	>10 MeV	10 MeV−1 GeV
Nuclear de-excitation lines	0.4,...,6.1 MeV	1-100 MeV/nucl.
Neutron capture line	2.2 MeV	1-100 MeV/nucl.
Positron annihilation radiation	0.511 MeV	1-100 MeV/nucl.
Pion decay radiation	10 MeV-3 GeV	0.2-5 GeV
Neutrons induced in atmospheric cascades	0.1-10 GeV	0.1-10 GeV
Neutron decay protons in space	20-200 MeV	20-400 MeV

emission at frequencies of $\nu \approx 300 - 700$ MHz during 13:42-13:50 UT (see Fig. 8 in Pohjolainen et al. 2001), a clear sign of gyro-synchroton radiation from trapped high-relativistic electrons during the GLE particle release time. The GLE event #58 on 1998 Aug 24, 22:05 UT, has the longest delay of $t_{SPR} - t_{HXR} = +26.2$ min, but the USAF/RSTN data (http://cdaw.gsfc.nasa.gov/meetings/lws-cdaw2009/data/White/) show a late increase of 15.4 GHz radio emission after 22:30 UT, which is an indicator of trapped high-relativistic electrons. The GLE event #61 on 2001 Apr 18, 02:12 UT, has a delay of $t_{SPR} - t_{HXR} = +10.9$ min, but this flare is occulted by 30^0 behind the limb, which may explain the offset timing because of the missed hard X-ray and soft X-ray peak. The GLE event #66 on 2003 Oct 29, 20:44 UT, has a delay of $t_{SPR} - t_{HXR} = +11.2$ min, but the USAF/RSTN data show very bursty radio spikes late in the flare during 20:50-20:56 UT at 610 MHz, a possible indication of a secondary acceleration phase producing electron beams in the lower corona. In summary, we observe in all cases with late GLE solar particle release times signs of extended particle acceleration or trapping, which does not exclude that the particles responsible for the GLE signatures have been accelerated and temporarily trapped (for $\approx 10 - 30$ min) at the solar flare site.

2.5 Maximum Energies of Solar Gamma Rays

There is no known high-energy cutoff of the electron bremsstrahlung spectrum; the highest energies of observed bremsstrahlung are around several 100 MeV (Forrest et al. 1985; Akimov et al. 1991, 1994a,b,c, 1996; Reames et al. 1992; Dingus et al. 1994; Trottet 1994; Kurt et al. 1996; Rank et al. 2001), see also reviews by Ramaty & Mandzhavidze (1994) or Chupp and Ryan (2009). Gamma-rays were reported up to energies above 1 GeV with the *Energetic Gamma-ray Experiment Telescope (EGRET)* on *CGRO* during the GLE event #51 on 1991 Jun 11 (Kanbach et al. 1992). The spectrum of the flare (Fig. 7) could be fitted with a composite of a proton generated pion neutral spectrum and a primary electron bremsstrahlung component (Kanbach et al. 1992). The GLE event #69 on 2005 Jan 20 reported gamma rays, protons, and pion decay radiation up to energies > 200 MeV (Grechnev et al. 2008). In Table 2 we list the energy ranges of observed photons in hard X-rays and gamma rays and the required primary particle energies for the various high-energy processes operating in large solar flares (adapted from Ramaty and Mandzhavidze 1994).

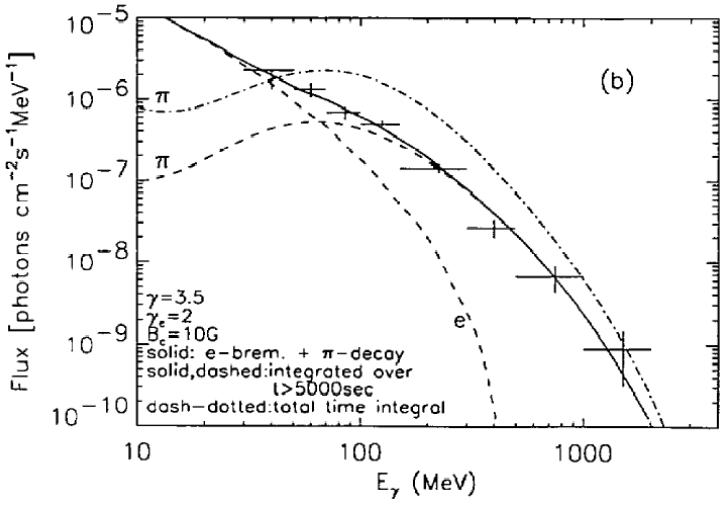

Fig. 7 A gamma-ray spectrum observed with *EGRET/CGRO* during the GLE event #51 on 1991 Jun 11, 02:04 UT flare, accumulated during 03:26−06:00 UT (Kanbach et al. 1993). The spectrum is fitted with a combination of primary electron bremsstrahlung and pion-decay radiation. Note that pion decay is dominant at energies $\gtrsim$ 40 MeV (Mandzhavidze & Ramaty 1992).

Do these highest observed energies constrain or rule out any acceleration mechanism? For DC electric field acceleration in sub-Dreicer fields, the maximum velocity to which electrons can be accelerated is limited by the value of the Dreicer field, which depends on the density and temperature of the plasma, $E_D \approx 2 \times 10^{-10} n/T$ (statvolts cm^{-1}). Holman (1996) argues that electron energies up to $10 - 100$ MeV can be attained for high densities of $n_e \approx 10^{12}$ cm^{-3} and low temperatures $T \approx 2$ MK (yielding a Dreicer field of $E_D = 1 \times 10^{-4}$ statvolt cm^{-1}, i.e., 3 V m^{-1}), if electrons are continuously accelerated over a current channel with a length of $L = 10 - 100$ Mm. The requirement for such large-scale DC electric fields, however, conflicts with the observed time-of-flight delays of hard X-ray pulses (e.g., Aschwanden et al. 1996) and the short inductive switch on/off time scales required for the observed subsecond hard X-ray pulses. Alternatively, Litvinenko (1996) envisions super-Dreicer electric fields, which can generate arbitrarily high maximum electron energies within much smaller spatial scales, and thus can be consistent with the time-of-flight delays of the observed hard X-ray pulses. The maximum energy for relativistic electrons obtained over an acceleration time t is approximately,

$$\varepsilon(t) = eEl(t) \approx eEct \ . \tag{5}$$

Litvinenko (2003) identifies plausible physical conditions with super-Dreicer fields of order $E \gtrsim 100$ V m^{-1} in reconnecting current sheets that lead to electron acceleration with gamma-ray energies of a few 10 MeV in electron-rich flares or to the generation of protons with energies up to several GeV in large gradual flares. A similar acceleration model was applied to the GLE event #59 on 2000 Jul 14 (Li et al. 2007). Also stochastic acceleration can generate 10 MeV electrons and 1 GeV protons (Miller et al. 1997), if a sufficiently high wave turbulence level is assumed (which, however, cannot easily be constrained by observations). Thus, the maximum observed gamma-ray energies imply

only constraints for the acceleration mechanism of sub-Dreicer electric DC fields, but not for super-Dreicer DC electric field, stochastic, or shock acceleration mechanisms.

3 Conclusions

The question whether the largest SEP and GLE events that accelerate ions with energies of $\gtrsim 1$ GeV are accelerated in solar flare regions or in interplanetary shocks, has been pondered for several decades. We review here *pro and con* aspects from the solar flare site that are relevant to answer this question, while the complementary aspects from CME-associated shocks are scrutinized in the companion article by Guang Li. The conclusions are based on observations of 70 GLE events over the last six decades, in particular on the 13 GLE events during the last solar cycle 23 (1998-2006) that provided excellent new imaging data in gamma rays and hard X-rays (RHESSI), in soft X-rays and EUV (TRACE, SOHO/EIT), and particle data from IMP, WIND, and ACE. Our conclusions are:

1. Solar particle release times t_{SPR} of GLE-producing particles overlap with the impulsive phase of gamma-ray and hard X-ray emission in solar flares in 9 out of 13 cases, and thus the acceleration time of GLE particles is consistent with the flare site in 70% of the cases.
2. The remaining cases, 4 our of 13 occur delayed to the flare peak by $\approx 10-30$ min, but observational signatures of extended acceleration and/or particle trapping is evident in all these cases, and thus 100% of the GLE events could be accelerated in flare sites. The alternative explanation of delayed second-step acceleration in CME-associated shocks cannot be ruled out for these 30% of the cases, possibly constituting a secondary gradual GLE component.
3. The height of the acceleration region of $\lesssim 1$ GeV electrons and ions depends on the interpretation, being $h \lesssim 0.05$ solar radii for flare site acceleration (according to electron time-of-flight measurements) or $h \approx 2-5$ solar radii for CME shock acceleration (according to type II source heights and GLE solar particle release delays).
4. The magnetic topology at the particle acceleration site is not well-known from magnetic modeling or tracing of coronal structures, but there is statistical evidence for open-field regions in most active regions that provide escape routes for GLE particles.
5. The recently discovered strong correlation between the spectral soft-hard-harder (SHH) evolution of solar hard X-rays and SEP events cannot be explained with the standard scenario of SEP acceleration in CME-associated shocks, and thus favors SEP acceleration in flare sites.
6. The maximum particle energies observed in solar flares reach up to several 100 MeV for electrons and above 1 GeV for ions. The required particle energies are $\lesssim 1$ GeV for the observed bremsstrahlung continuum at photon energies of $\lesssim 10$ MeV, and $0.2-5$ GeV for pion decay radiation observed at photon energies of 10 MeV -3 GeV, which is sufficient to explain GLE detections.
7. Energies up to $\lesssim 1$ GeV can be achieved for DC electric field acceleration in super-Dreicer fields, for stochastic acceleration, and for shock acceleration. Only DC electric field acceleration in sub-Dreicer fields can be ruled out, based on the large distances of DC fields required and the inconsistent electron time-of-flight delays.

What progress do we need to answer the question about the origin of GeV particles with more certainty? The velocity dispersion measurements with IMP, WIND, and ACE helped enormously to narrow down the start window of solar particle release times, which could be even more constrained with the particle detectors PLASTIC and IMPACT on STEREO. The most sensitive hard X-ray and gamma-ray detectors existed on CGRO, but in near future we have only RHESSI available. However, RHESSI provides excellent imaging capabilities, which revealed intriguing information on displaced electron and ion acceleration sites in the solar corona (Hurford et al. 2003, 2006). In addition we expect also improved magnetic modeling of solar flare regions that can reveal open-field and closed-field geometries with more certainty, using nonlinear force-free field (NLFFF) codes (e.g., Bobra et al. 2008; DeRosa et al. 2009) with 3-D vector magnetograph data from the *Solar Dynamics Observatory (SDO)*, possibly in conjuction with stereoscopic 3-D reconstruction of flaring active regions using *STEREO/EUVI*.

Acknowledgements This work resulted from two Coordinated Data Analysis Workshops (CDAW) on Ground Level Enhancement Events (GLEs), held in January 2009 in Palo Alto, California, and in November 2009, Huntsville, Alabama, organized by Nariaki Nitta and Nat Gopalswamy.

References

Akimov, V.V. and 33 co-authors 1991, in Proc. 22nd Internat. Cosmic Ray Conference, Internat. Union of Pure and Applied Physics (IUPAP), The Institute for Advanced Studies: Dublin, Vol. 3, p. 73.

Akimov, V.V., Belov, A.V., Chertok, I.M., Kurt, V.G., Leikov, N.G., Magun, A., and Melnikov, V.F. 1994a, Proc. Kofu Symposium, Kofu, Japan, p.371.

Akimov, V.V., Leikov, N.G., Belov, A.V., Chertok, I.M., Kurt, V.G., Magun, A., and Melnikov, V.F. 1994b, in *High-energy solar phenomena - A new era of spacecraft measurements* (eds. Ryan, J. and Vestrand, W.T.), American Institute of Physics: New York, p.106.

Akimov, V.V., Leikov, N.G., Kurt, V.G., and Chertok, I.M. 1994c, in *High-energy solar phenomena - A new era of spacecraft measurements* (eds. Ryan, J. and Vestrand, W.T.), American Institute of Physics: New York, p.130.

Akimov, V.V., Ambroz, P., Belov, A.V., Berlicki, A., Chertok, I.M., Karlicky, M., Kurt, V.G., Leikov, N.G., Litvinenko, Y.E., Magun, A., Minko-Wasiluk, A., Rompolt, B., and Somov, B.V. 1996, Solar Phys. 166, 107.

Aschwanden, M.J., Kosugi, T., Hudson, H.S., Wills, M.J., and Schwartz, R.A. 1996, ApJ 470, 1198.

Aschwanden, M.J. and Alexander, D. 2001, SP 204, 91.

Aschwanden, M.J. 2002, Space Science Reviews 101, 1.

Aschwanden, M.J. 2004 (1st Edition; 2005 paperback), *Physics of the Solar Corona - An Introduction*, Praxis Publishing Ltd., Chichester UK, and Springer, New York.

Aschwanden, M.J. and Aschwanden, P.D. 2008, ApJ 674, 530.

Aulanier, G., DeLuca, E.E., Antiochos, S.K., McMullen, R.A. and Golub, L. 2000, Astrophys. J.540, 1126.

Bieber, J.W., Clem,J., Evenson, P., Pyle, R., Ruffolo, D., Saiz, A., and Wechakama, M. 2008, in Proc. 30th Internat. Cosmic Ray Conf. (eds. Caballero et al.), Universidata Nacional Autonoma de Mexico, Mecico, p.229-232.

Bobra, M.G., VanGallegooijen, A.A., and DeLuca, E.E. 2008, Astrophys. J.672, 1209.

Bombardieri, D.J., Duldig, M.L., Humble, J.E., and Michael, K.J. 2008, ApJ 682, 1315.

Chertok, I.M. 1995, in 24th Internat. Cosmic Ray Conference, (eds. Iucci, N. and Lamanna,E.), Internat. Union of Pure and Applied Physics, Vol. 4, p.78.

Chupp, E.L., and Ryan, J.M. 2009, Research in Astron. Astrophys. 9/1, 11.

Cliver, E.W., Kahler, S.W., Shea, M.A., and Smart, D.F. 1982, ApJ 260, 362.

Cliver, E.W. 2006, ApJ 639, 1206.

Dennis, B.R. and Zarro, D.M. 1993, SP 146, 177.

DeRosa, M.L., Schrijver, C.J., Barnes, G., Leka, K.D., Lites, B.W., Aschwanden, M.J., Amari, T., Canou, A., McTiernan, J.M., Regnier, S., Thalmann, J., Valori, G., Wheatland, M.S., Wiegelmann, T., Cheung, M.C.M., Conlon, P.A., Fuhrmann, M., Inhester, B., and Tadesse, T. 2009, Astrophys. J.696, 1780.

Dingus, B.L., Sreekumar, P., Bertsch, D.L., Schneid, E.J., Brazier, K.T.S., Kanbach, G., von Montigny, C., Mayer-Hasselwander, H.A., Lin, Y.C., Michelson, P.F., Nolan, P.L., Kniffen, D.A., Mattox, J.R. 1994, in *High-energy solar phenomena - A new era of spacecraft measurements* (eds. Ryan, J. and Vestrand, W.T.), American Institute of Physics: New York, p.177.

Forbes, T.G. and Priest, E.R. 1995, ApJ 446, 377.

Forrest, D.J., Vestrand, W.T., Chupp, E.L., Rieger, E., Cooper, J.F., and Share, G.H. 1985, in 19th Intern. Cosmic Ray Conf., NASA Goddard Space Flight Center: Greenbelt, Maryland, Vol. 4., p.146.

Gopalswamy, N., Xie, Hl, Yashiro, S., and Usoskin, I. 2008, Indian J. Radio and Space Physics (in press).

Grayson, J.A., Krucker, S., and Lin, R.P. 2009, Astrophys. J.707, 1588.

Grechnev, V,V, Kurt, V.G., Chertok, I.M., Uralov, A.M., Nakajima, H., Altyntsev, A.T., Belov, A.V., Yushkov, B.Yu., Kuznetsov, S.N., Kashapova, L.K., Meshalkina, N.S., and Prestage, N.P. 2008, Solar Phys. 252, 149.

Holman, G.D. 1996, in *High Energy Solar Physics*, (eds. Ramaty, R., Mandzhavidze, N., and Hua, X.-M.), American Institute of Physics: Woodbury, New York, Conf. Proc. 374, p.479.

Hudson, H.S. 1991, BAAS 23, 1064.

Hurford, G.J., Schwartz, R.A., Krucker, S., Lin, R.P., Smith, D.M., and Vilmer, N. 2003, Astrophys. J.595, L77.

Hurford, G.J., Krucker, S., Lin, R.P., Schwartz, R.A., Share, G.H., and Smith, D.M. 2006, Astrophys. J.644, L93.

Kanbach, G., Bertsch, D.L., Fichtel, C.E., Hartman, R.C., Hunter, S.D., Kniffen, D.A., Kwok, P.W., Lin, Y.C., Mattox, J.R., and Mayer-Hasselwander, H.A. 1992, in *EGRET Mission and Data Analysis*, Technical Report N94-19462 04-89, Max-Planck-Inst. für Physik und Astrophysik: Munich, p.5.

Kanbach, G, Bertsch, D.L., Fichtel, C.E., Hartman, R.C., Hunter, S.D., Kniffen, D.A., Kwok, P.W., Lin, Y.C., Mattox, J.R. and Mayer-Hasselwander, H.A. 1993, AASS 97, 349.

Karpen, J.T., Antiochos, S.K., and DeVore, C.R. 1995, ApJ 450, 422.

Karpen, J.T., Antiochos, S.K., DeVore, C.R.,a nd Golub, L. 1998, ApJ 495, 491.

Kiplinger, A.L. 1995, Astrophys. J.453, 973.

Klassen, A., Krucker, S., Kunow, H., Müller-Mellin, R., Wimmer-Schweingruber, R. 2005, JGR 110, A09S04.

Klein, K. and Trottet, G. 2001, American Geophysical Union, Meeting abstract #SH31C-09.

Kliem, B., Karlicky, M., and Benz, A.O. 2000, A&A 360, 715.

Kocharov, L., Klein, K.-L., Saloniemi, O., Kovaltsov, G., and Torsti, J. 2006, 36th COSPAR Scientific Assembly, Meeting abstract #2897.

Kundu, M.R. 1965, *Solar Radio Astronomy*, Wiley: New York.

Kurt, V.G., Akimov, V.V., and Leikov, N.G. 1996, in *High Energy Solar Physics*, (eds. Ramaty, R., Mandzhavidze, N., and Hua, X.-M.), American Institute of Physics: Woodbury, New York, Conf. Proc. 374, p.237.

Kuznetsov, S.N., Kurt, V.G., Yushkov, B.Y., Myagkova, I.N., Kudela, K., Kassovicova, J., and Slivka, M. 2006, Contrib. Astron. Obs. Skalnaté Pleso 36, 85.

Li, J., Tang, Y.H., Dai, Y., Zong, W.G., and Fang, C. 2007, A&A 461, 1115.

Li, J., Dai, Y., Vial, J.C., Owen, C.J., Matthews, S.A., Tang, Y.H., Fang, C., Fazakerley, A.N. 2009, A&A 503, 1013.

Litvinenko, Y.E. 1996, Astrophys. J.462, 997.

Litvinenko, Y.E. 2003, Solar Phys. 216, 189.

Livshits, M.A. and Belov, A.V. 2004, Astronomy Reports 48/8, 665.

Mandzhavidze, N. and Ramaty, R. 1992, Astrophys. J.389, 739.

Martirosyan, H. and Chilingarian, A. 2005, Proc. 29th Internat. Cosmic Ray Conf. (eds. Acharya, B.S. et al.), Tata Institute of Fundamental Research: Mumbai, Vol.2, p.285.

Masson, S. and Klein, K.-L. 2009, RHESSI nugget, http:/sprg.ssl.berkeley.edu/~ tohban/wiki/index.php/ Solar_Cosmic_Rays_of_the_GLE_on_20_January_2005

Masuda, S. 2002, in *Multi-wavelength observations of coronal structure and dynamics - Yohkoh 10th Anniversary Meeting*, (eds. Martens, P.C.H. and Cauffman, D.), COSPAR Coll. Series, Elsevier, p.351.

Masuda, S., and Sato, J. 2003, Adv. Space Res. 32/12, 2455.

Matthiä, D., Heber, B., Reitz, G., Meier, M., Sihver, L., Berger, T., and Herbst K. 2009, J. Geophys. Res. 114/A8, CiteID A08104.

McCracken, K.G. and Moraal, H. 2008, in Proc. 30th Internat. Cosmic Ray Conf. (eds. Caballero et al.), Universidata Nacional Autonoma de Mexico, Mecico, p.269.

McCracken, K.G., Moraal, H., and Stoker, P.H. 2008, JGR 113, A12101.

Miller, J.A., Cargill, P.J., Emslie, A.G., Holman, G.D., Dennis, B.R., LaRosa, T.N., Winglee, R.M., Benka, S.G., and Tsuneta, S. 1997, JGR 102/A7, 14631.

Miroshnichenko, L.I., Klein, K.-L., Trottet, G., Lantos, P., Vashenyk, E.V., and Balabin, Y.V. 2004, 35th COSPAR Scientific Assembly, Meeting abstract #2225.

Moraal, H., McCracken, K.G., and Stoker, P.H. 2008, in Proc. 30th Internat. Cosmic Ray Conf. (eds. Caballero et al.), Universidata Nacional Autonoma de Mexico, Mecico, p.265.

Murphy, R.J., Share, G.H., Schwartz, R.A., Yoshimori, M., Suga, K., Nakayama, S., Takeda, H. 2001, American Geophysical Union, Meeting abstract #SP42A-10.

Neupert, W.M. 1968, ApJ 153, L59.

Pohjolainen, S., Maia, D., Pick, M., Vilmer, N., Khan, J.I., Otruba, W., Warmuth, A., Benz, A., Alissandrakis, C., and Thompson, B.J. 2001, Astrophys. J.556, 421.

Ramaty, R. and Mandzhavidze, N. 1994, in *High-energy solar phenomena - A new era of spacecraft measurements* (eds. Ryan, J. and Vestrand, W.T.), American Institute of Physics: New York, p.26.

Rank, G., Bennett, K., Bloemen, H., Debrunner, H., Lockwood, J., McConnell, M., Ryan, J., Schönfelder, V., and Suleiman, R. 1996, in *High Energy Solar Physics*, AIP Conf. Proc. 374, (eds. Ramaty, R., Mandzhavidze, N., and Hua, X.-M.), American Institute of Physics: New York, p.219.

Rank, G., Ryan, J., Debrunner, H., McConnell, M., and Schoenfelder, V. 2001, A&A 378, 1046.

Reames, D.V., Richardson, I.G., and Wenzel, K.P. 1992, Astrophys. J.387, 715.

Reames, D.V. 2002, Astrophys. J.571, L63.

Reames, D.V. 2009a, ApJ 693, 812.

Reames, D.V. 2009b, ApJ 706, 844.

Schrijver, C.J. and DeRosa, M.L. 2003, Solar Phys.212, 165.

Shibata, K. and Tanuma, 2001, Earth, Planets and Space 53, 473.

Shumilov, O.I., Kasatkina, E.A., Turyansky, V.A., Kyro, E., Kivi, R. 2003, Adv. Space Res. 31/9, 2157.

Simnett, G.M. 2006, A&A 445, 715.

Simnett, G.M. 2007, (Erratum) A&A 472, 309.

Simnett, G.M. and Roelof, E.C. 2005a, 29th Internat Cosmic Ray Conf. 1, 233.

Simnett, G.M. and Roelof, E.C. 2005b, AGU Meeting abstract #SH23A-0319.

Sturrock, P.A. 1966, Nature 5050, 695.

Torsti, J., Riihonen, E., and Kocharov, E. 2004, ApJ 600, L83.

Trottet, G. 1994, in *High-energy solar phenomena - A new era of spacecraft measurements* (eds. Ryan, J. and Vestrand, W.T.), American Institute of Physics: New York, p.3.

Vashenyk, E.V., Balanin, Y.V., and Gvozdevsky, B.G. 2003, 28th Internat. Cosmic Ray Conf., p.3401.

Wang, H., Gary, D.E., Zirin, H., Schwartz, R.A., Sakao, T., Kosugi, T., and Shibata, K., 1995, ApJ 453, 505.

Wang, R.G. and Wang, J.X. 2006, 36th COSPAR Scientific Assembly, Meeting abstract #1856.

Wang, R.G. 2009, Astroparticle Physics 31/2. 149.

Watanabe, K., Murphy, R.J., Share, G.H. et al. 2008, in Proc. 30th Internat. Cosmic Ray Conf. (eds. Caballero et al.), Universidata Nacional Autonoma de Mexico, Mecico, p.41.

Yan, Y. and Huang, G. 2003, Space Science Rev. 107, 111.